

Interdecadal changes in the relationship between Southern China winter-spring precipitation and ENSO

Jiepeng Chen · Zhiping Wen · Renguang Wu ·
Zesheng Chen · Ping Zhao

Received: 5 May 2013 / Accepted: 14 September 2013 / Published online: 22 September 2013
© Springer-Verlag Berlin Heidelberg 2013

Abstract Winter-spring precipitation in southern China tends to be higher (lower) than normal in El Niño (La Niña) years during 1953–1973. The relationship between the southern China winter-spring precipitation and El Niño–Southern Oscillation (ENSO) is weakened during 1974–1994. During 1953–1973, above-normal southern China rainfall corresponds to warmer sea surface temperature (SST) in the equatorial central Pacific. There are two anomalous vertical circulations with ascent over the equatorial central Pacific and ascent over southern China and a common branch of descent over the western North Pacific that is accompanied by an anomalous lower-level anticyclone. During 1974–1994, above-normal southern China rainfall corresponds to warmer SST in eastern South Indian Ocean and cooler SST in western South Indian Ocean. Two anomalous vertical circulations act to link southern China rainfall and eastern South Indian Ocean SST anomalies, with ascent over eastern South Indian Ocean and southern China and a common branch of descent over the western North Pacific. Present analysis shows that South Indian Ocean SST anomalies can contribute to southern China winter-spring precipitation variability independently. The observed change in the relationship

between southern China winter-spring rainfall and ENSO is likely related to the increased SST variability in eastern South Indian Ocean and the modulation of the Pacific decadal oscillation.

Keywords Interdecadal changes · Southern China winter-spring precipitation–ENSO relationship · South Indian Ocean SST

1 Introduction

Most of previous studies focus on summer rainfall in China because of the large impacts of summer flood and drought. Although winter precipitation in southern China accounts for about 10–15 % of the annual total rainfall (Wang and Feng 2011), with the development of society and economy, people start to pay attention to winter climate and its effects on agriculture, manufacture, water resource, energy, etc. The forecasting of winter precipitation is set as an important service in China Meteorological Administration (He et al. 2007). Winter-spring rainfall anomalies may cause severe disaster. For example, southern China suffered from unprecedented severe climate from January to early February 2008 when low temperature, glaze, and heavy snowfall struck the transportation, communication and electricity transmission lines (Gao et al. 2008; Wang et al. 2008a, b; Zhao et al. 2008; Ma 2009; Wen et al. 2009; Zhang et al. 2009; Zhou et al. 2011). In southern China, spring rainfall accounts for about 30–40 % of annual total rainfall, and the mean and the standard deviation of rainfall in spring is close to that in summer (Wu et al. 2003). Spring runoff in east China (including southern China) responds directly to simultaneous local rainfall, which is quite different from that in summer (Chen et al. 2009). Southern

J. Chen · Z. Wen (✉) · Z. Chen
Center for Monsoon and Environment Research and Department
of Atmospheric Sciences, Sun Yat-Sen University,
Guangzhou 510275, China
e-mail: eeswzp@mail.sysu.edu.cn

R. Wu
Institute of Space and Earth Information Science and
Department of Physics, The Chinese University of Hong Kong,
Shatin, Hong Kong SAR, China

P. Zhao
Chinese Academy of Meteorological Sciences, Beijing, China

China is densely populated and is an important economic region of China. Anomalous rainfall in winter and spring has large impacts on economics and people's lives. Thus, understanding the causes and improving the forecasts of southern China winter-spring precipitation will have great benefits to the society and economy.

The variability of southern China rainfall in winter and spring has been attributed to influences of various factors, including El Niño-Southern Oscillation (ENSO) (Zhang et al. 1996, 1999; Wang et al. 2000; Wu et al. 2003; Zhang and Sumi 2002; Zhou and Wu 2010; Wang and Feng 2011, Sun and Yang 2012), sea surface temperature (SST) in the South China Sea (Zhou et al. 2010) and the Indian Ocean (Yang 2009), the Tibetan Plateau snow cover (Chen and Yan 1979; Chen and Wu 2000; Wu and Kirtman 2007a) or thermal condition (Liu and Wang 2011; Sun and Yang 2012), the Arctic Oscillation (Yang 2011) and the North Atlantic Oscillation (Sun and Yang 2012). The Arctic Oscillation or North Atlantic Oscillation can affect southern China winter-spring rainfall through modulating the East Asian winter monsoon (EAWM) (Wu and Huang 1999; Gong et al. 2001; Wu and Wang 2002a, b; Sung et al. 2010).

Anomalous winter and spring rainfall in southern China has been linked to the strength of cold northerly and warm southwesterly that may induce convergence and divergence over southern China. The low-latitude circulation systems that can affect southern China rainfall include the western Pacific subtropical high (Zhang et al. 1996; Wang et al. 2000; Wu et al. 2003) and the trough over the Bay of Bengal (Wang et al. 2011; Zong et al. 2012). These circulation systems can enhance or reduce the transport of moisture to southern China, leading to more or less precipitation. Li et al. (2010) pointed out that the transport of water vapor from the Bay of Bengal favors winter and spring rainfall in southern China. The western Pacific subtropical high can act as a medium for ENSO's influence on East Asian climate (Wang et al. 2000; Huang et al. 2012).

Previous studies are mostly concerned with rainfall anomalies in individual seasons. This study considers winter and spring rainfall together since persistent rainfall anomalies have larger impacts. For example, more than 98.9 million hectares of crops were destroyed and more than 4.9 million people and 3.4 million livestock were short of drinking water because persistent severe drought in southern China from the peak winter to the late spring in 2011 (Sun and Yang 2012).

Sun and Yang (2012) investigated the ENSO impacts on persistent drought from winter to spring in southern China. Wu et al. (2012) identified an interdecadal change in the relationship between southern China summer rainfall and tropical Indo-Pacific SST. Is there interdecadal change in the ENSO impacts on winter-spring rainfall in southern

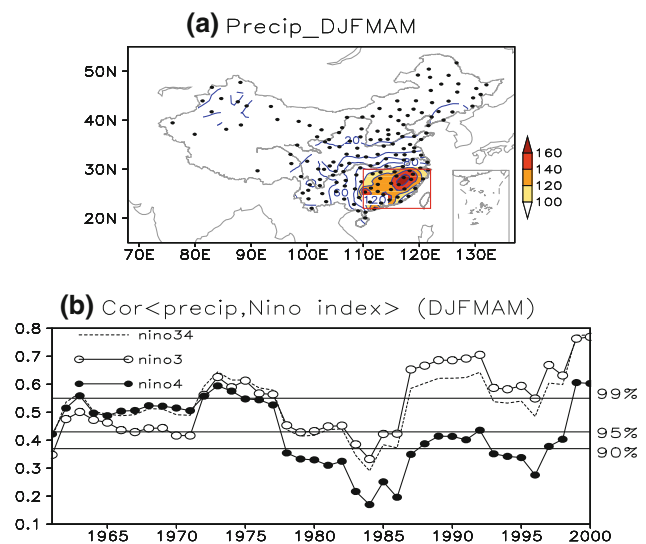


Fig. 1 **a** Station locations (black dots) and averaged monthly rainfall (mm/month) in southern China during DJFMAM 1951–2010 from station data. The rectangle denotes the location of southern China (22°–30°N and 110°–122°E, 27 stations). Contour interval is 20 mm/month. Shading indicates rainfall over 100 mm/month. **b** Moving correlation coefficient of NINO3.4 (dash line), NINO3 (open circle) and NINO4 (solid circle) DJFMAM SST with southern China DJFMAM rainfall with a 21-year window. The correlation is shown at the center year of the 21-year window

China? Our analysis shows that the relationship between southern China winter-spring rainfall and ENSO is weakened around the mid-1970s (Fig. 1b). Wet winter-springs occurred frequently in southern China during the El Niño years before the mid-1970s, whereas southern China winter-spring rainfall displayed a weak positive correlation with ENSO after the mid-1970s. Why has the relationship between southern China winter-spring rainfall and ENSO changed since the mid-1970s? What are the factors for southern China dry winter-springs after the mid-1970s given the weakened ENSO impact? What are the circulation features associated with southern China dry winter-springs before and after the mid-1970s, respectively? These are the questions to be addressed in this study.

The main purpose of the present study is to investigate and understand interdecadal changes in the relationship between southern China winter-spring rainfall and ENSO. The rest of the paper is organized as follows. The datasets, methods, and model used in the present study are described in Sect. 2. The interdecadal change in the relationship of southern China winter-spring rainfall with SST and atmospheric circulation is documented in Sect. 3. Section 4 uses conditional composite analysis to unravel the independent influence of the South Indian Ocean SST anomalies. The plausible causes for the interdecadal change in southern China winter-spring rainfall–SST relationship are discussed in Sect. 5. Section 6 presents the summary of the results.

2 Datasets, methods, and model

The rainfall used in the present study is monthly rainfall of 160 stations in China from 1951 to 2011, which is obtained from the National Climate Center of the China Meteorological Administration. The southern China winter-spring (December–May or DJFMAM in short) precipitation is defined as the average of rainfall at 27 stations located to the east of 110°E and from 22°N to 30°N. The station locations along with climatological winter-spring rainfall during 1951–2010 are shown in Fig. 1a. The present study uses the NOAA Extended Reconstruction monthly mean SST, version 3 (Smith et al. 2008), which is available on 2.5° grid from 1854 to present, from its website at <http://www.esrl.noaa.gov/psd/data/gridded/data.noaa.ersst.html>. Hadley Centre's sea ice and SST (HadISST) (Rayner et al. 2003) is also used in this study. The monthly mean winds and vertical velocity are provided by the National Centers for Environmental Prediction–National Center for Atmospheric Research (NCEP–NCAR) reanalysis product (Kalnay et al. 1996), which are available on 2.5° grid from 1948 to present and obtained from its website at <http://www.esrl.noaa.gov/psd/data/gridded/data.ncep.reanalysis.html>. The velocity potential and divergent winds are derived from winds. The monthly Pacific decadal oscillation (PDO) index is obtained from <http://jisao.washington.edu/pdo/PDO.latest> derived as the leading PC of monthly SST anomalies in the North Pacific Ocean, poleward of 20°N.

There may be unrealistic interdecadal variability in the NCEP–NCAR reanalysis (Yang et al. 2002; Inoue and Matsumoto 2004; Wu et al. 2005). This study focuses on the interannual variations, so variations with periods of 8 years and longer have been removed using a harmonic analysis in order to avoid plausible contamination of interannual relationship by interdecadal changes. This approach is applied following Wu et al. (2010, 2012). The relationships between pairs of variables are examined by correlation and composite analyses and the statistical significance of these analyses are assessed using the two sided Student's *t* test.

As this study is concerned with persistent rainfall anomalies during winter through spring, we consider the winter and spring rainfall anomalies together in constructing an area-mean rainfall index for southern China. Due to the fact that the rainfall amount and its variability is several times larger in spring than in winter in southern China, we have normalized the monthly rainfall anomalies before the construction of December through May (DJFMAM) mean rainfall index. The correlation coefficients between the winter-spring rainfall index and monthly rainfall from December to May are 0.51, 0.62, 0.41, 0.35, 0.45, and 0.51, respectively. All these correlation coefficients reach the 99 % confidence level according to the

Student's *t* test. The magnitude of these correlation coefficients, however, is not very high. This indicates that there are both years when the winter and spring rainfall anomalies are of the same sign (persistent anomalies) and years when they are not (non-persistent anomalies), which is expected. By considering the winter and spring rainfall anomalies together in constructing the rainfall index, this study is concerned with those years when rainfall anomalies persist from winter to spring, but not those years with non-persistent anomaly years, which differs from most of previous studies. Also, because the analysis is based on the winter-spring rainfall index, we are looking for the factors that contribute to persistent rainfall anomalies.

The National Center for Atmospheric Research (NCAR) Community Atmospheric Model version 4.0 (CAM4) with monthly SST from the HadISST dataset with a horizontal resolution of 1° in both latitude and longitude (Rayner et al. 2003) is used. The CAM 4.0 is the sixth generation of the NCAR atmospheric global climate model and has been developed through a collaborative process of users and developers in the atmosphere model working group with significant input from the chemistry climate working group and the whole atmosphere model working group (Neale et al. 2011). CAM4 is part of the community climate system model (CCSM4) and contains a number of notable improvements including dynamical core, resolution changes, deep convection and cloud fraction compared to CAM3 (http://www.cesm.ucar.edu/models/ccsm4.0/notable_improvements.html).

3 Interdecadal change in the relationship between southern China winter-spring precipitation and ENSO

The winter-spring rainfall amounts is larger than 60 mm/month in the southern part of China and less than 60 mm/month to north of Yangtze River and in western part of China (Fig. 1a). In this study, we focus on southern China rainfall where winter-spring rainfall amount is greater than 100 mm/month. Figure 1b shows the sliding correlation of southern China winter-spring rainfall and SST anomalies in the NINO3 (5°S–5°N, 90°–150°W), NINO3.4 (5°S–5°N, 170°–120°W), and NINO4 (5°S–5°N, 160°E–150°W) regions with a window of 21-year. The sliding correlation for NINO3.4 SST falls between those for NINO3 and NINO4 SSTs. The sliding correlation before mid-1970s is significantly positive for NINO3 and NINO4 SSTs. An obvious drop in the correlation is seen in the late 1970s. The weak correlation for NINO4 SST maintains to the late 1990s, after which the correlation recovers. The correlation for NINO3 SST displays an earlier recovery in the late 1980s. The correlation for NINO3.4 SST shows more obvious interdecadal changes than that for NINO3 SST.

Consistent results are obtained when the sliding correlation is calculated based on the SST from Hadley Centre's sea ice and SST data set (figure not shown). Because the atmospheric response to SST anomalies depends upon the background SST, here, we focus on the correlation for NINO4 SST. The 21-year sliding correlation is the most and least significant in years 1963 and 1984, respectively. Thus, we choose 1953–1973 and 1974–1994 as the two sub-periods in the following correlation and regression analyses to comprehend the change in the relationship between southern China winter-spring rainfall and equatorial central Pacific SST. The correlation coefficient in 1953–1973 is +0.56 for NINO4 SST, which is significant at the 99 % confidence level according to the Student's *t* test. The correlation coefficient in 1974–1994 is +0.17 for NINO4 SST, which is below the 90 % confidence level. During 1953–1973, there are seven (nine) years in which southern China winter-spring rainfall is above-normal (below-normal) corresponding to positive (negative) NINO4 SST, whereas there are 5 years in which NINO4 SST and southern China winter-spring anomalies are of the opposite signs. During 1974–1994, there are six (five) years in which southern China winter-spring rainfall is above-normal (below-normal) corresponding to positive (negative) NINO4 SST, whereas there are 10 years in which NINO4 SST and southern China winter-spring anomalies are of the opposite signs. The above statistics confirms the weakening of the relationship between southern China winter-spring rainfall and equatorial central Pacific SST around the mid-1970s.

To understand the interdecadal change in the relationship between southern China winter-spring precipitation and ENSO, we show in Fig. 2 SST anomalies in DJFMAM obtained by regression onto normalized southern China winter-spring rainfall anomalies for the two sub-periods separately. There are several notable differences between the periods 1953–1973 and 1974–1994. First, positive SST anomalies in the equatorial central Pacific are significant and large during 1953–1973, whereas they are small and insignificant during 1974–1994. Second, positive SST anomalies extend from tropical Indian Ocean to the South China Sea during 1953–1973, whereas the SST anomalies are weak in these regions during 1974–1994 except for southeastern tropical Indian Ocean. Third, there is an SST anomaly dipole in the South Indian Ocean during 1974–1994, with large significant positive SST anomalies in the east and significant negative SST anomalies in the west, respectively. This SST anomaly pattern resembles the leading Indian Ocean SST mode obtained by Xu and Fan (2012). We will discuss the implication of these differences further.

To understand the connection of southern China winter-spring rainfall to the equatorial central Pacific SST and

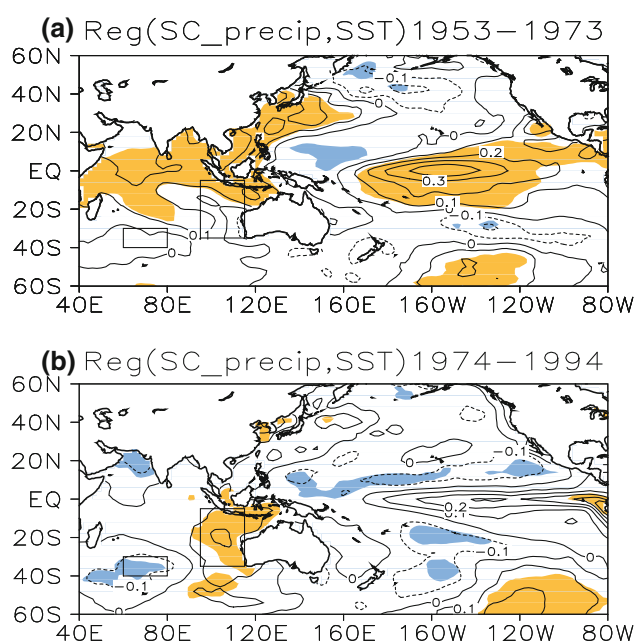


Fig. 2 SST anomalies in DJFMAM obtained by regression on normalized southern China DJFMAM rainfall during 1953–1973 (a) and 1974–1994 (b). Contour interval is 0.1 °C. Shading denotes the corresponding correlation coefficient larger than 0.433, which is significant at the 95 % confidence level

South Indian Ocean SST, we show in Fig. 3 anomalous winds at 850 and 200 hPa and in Fig. 4 vertical velocity at 500 hPa obtained by regression on normalized southern China winter-spring rainfall. At 850 hPa (Fig. 3a, b), there is an anomalous anticyclone over the western North Pacific. Anomalous southwesterly winds along the western flank of the anomalous anticyclone enhance the moisture supply to southern China (Zhang et al. 1996; Wang et al. 2000). Westerly anomalies blow from equatorial central to eastern Pacific. At 200 hPa (Fig. 3c, d), an anomalous cyclone controls the western North Pacific. Anomalous easterlies are observed over the equatorial central Pacific with two anomalous anticyclones lying to the south and north of the equator (Fig. 3c). At 500 hPa (Fig. 4a, b), there is anomalous upward motion over the equatorial central Pacific, downward motion over the western North Pacific, and upward motion over southern China, respectively. The anomalous anticyclonic winds over the western North Pacific are robust around the mature phase of ENSO, as have been pointed out by previous researches (Wang et al. 2000, 2003; Wu et al. 2003). The generation and development of the western North Pacific anticyclone is not only related to large SST anomalies in the equatorial central-eastern Pacific (Wang et al. 2000), but also to local SST anomalies in the western North Pacific (Wu and Wang 2000). Anomalous heating over the equatorial central Pacific induced by warm SST anomalies lead to downward motion over the western North Pacific and low-level

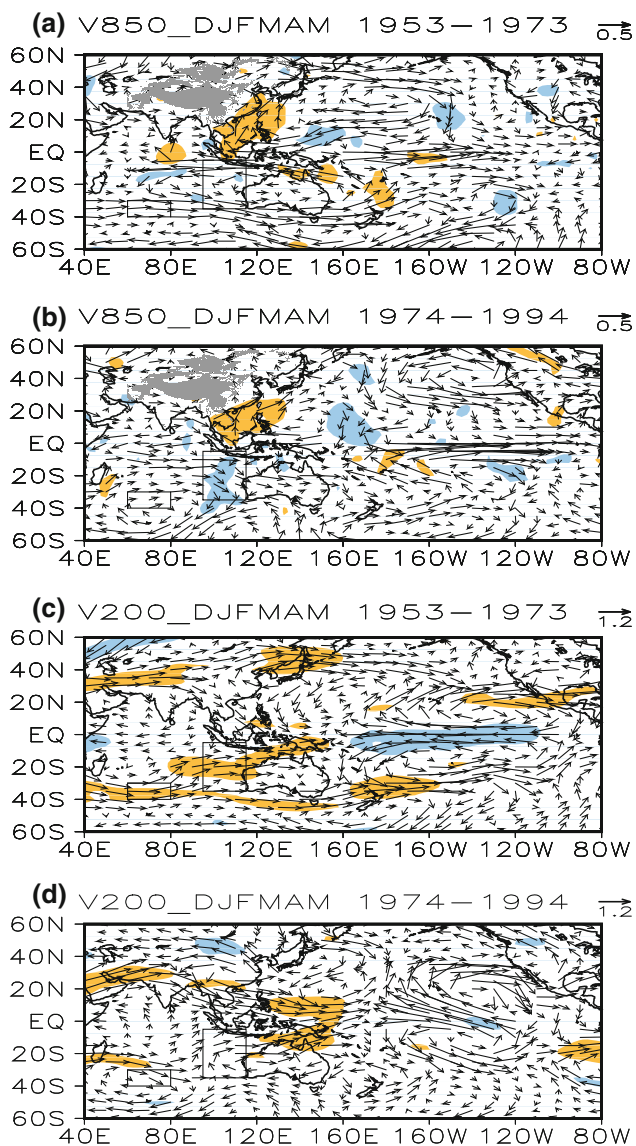


Fig. 3 Anomalies of 850 hPa winds (a, b) and 200 hPa winds (c, d) in DJFMAM obtained by regression on normalized southern China DJFMAM rainfall during 1953–1973 (a, c) and 1974–1994 (b, d). The wind scale is shown at the top of the respective panels. Shading denotes the corresponding correlation coefficient larger than 0.433, which is significant at the 95 % confidence level

anticyclone (Wang et al. 2000; Wu and Wang 2000). The low-level anticyclone is maintained through in situ air-sea interaction (Wang et al. 2000).

Notable difference in wind anomalies is seen over the South Indian Ocean. During 1953–1973, an anomalous anticyclone controls the tropics at 850 hPa (Fig. 3a), which is overlaid by anomalous wind convergence at 200 hPa (Fig. 3c) and downward motion at 500 hPa (Fig. 4a). In contrast, during 1974–1994, an anomalous cyclone dominates most of the tropics at 850 hPa (Fig. 3b), which is overlaid by anomalous wind divergence at 200 hPa

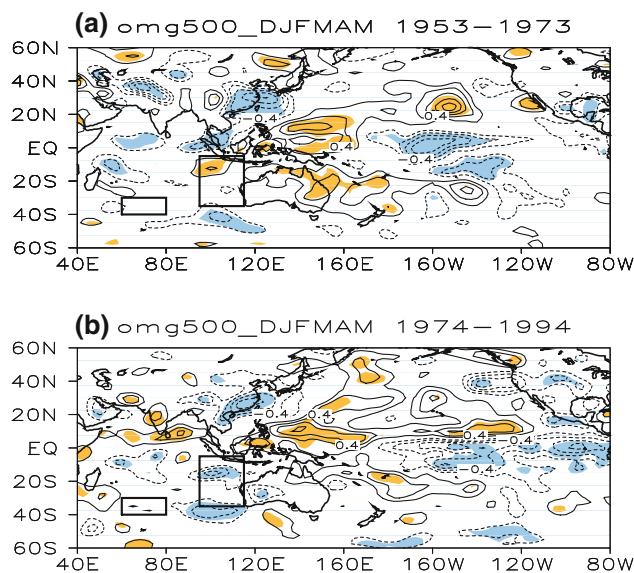


Fig. 4 500 hPa p-vertical velocity anomalies in DJFMAM obtained by regression on normalized southern China DJFMAM rainfall during 1953–1973 (a) and 1974–1994 (b). The zero contour is suppressed. Contour interval is 0.002 Pa/s. Shading denotes the corresponding correlation coefficient larger than 0.433, which is significant at the 95 % confidence level

(Fig. 3d) and upward motion at 500 hPa (Fig. 4b). The 500 hPa vertical motion anomalies over the western North Pacific and eastern tropical Indian Ocean form a southwest-northeast contrast during 1974–1994 (Fig. 4b).

The correspondence between SST and vertical motion anomalies over eastern tropical South Indian Ocean indicates a change in the air-sea relationship. During 1953–1973, warmer SST corresponds to anomalous downward motion. As such, it appears that the ocean responds to the atmosphere. The suppression of cloud and associated increase in downward shortwave radiation leads to SST warming (Wu and Kirtman 2007b). The anomalous descent may be attributed to remote forcing from the equatorial central and eastern Pacific. In contrast, during 1974–1994, anomalous cyclonic winds and ascent appear to be responses to local positive SST anomalies. Why does the atmosphere–ocean relationship change in the mid-1970s? This may be related to the change in the magnitude of SST anomalies in the eastern tropical South Indian Ocean, which will be discussed in Sect. 5.

The lower-level and upper-level anomalous winds indicate a close connection between the atmospheric circulation over southern China and that over equatorial central Pacific or the South Indian Ocean. In order to further demonstrate the above connection, we examine the anomalies of velocity potential at 200 and 850 hPa with respect to normalized southern China winter-spring rainfall. During 1953–1973, there is anomalous divergence over equatorial central Pacific, anomalous convergence

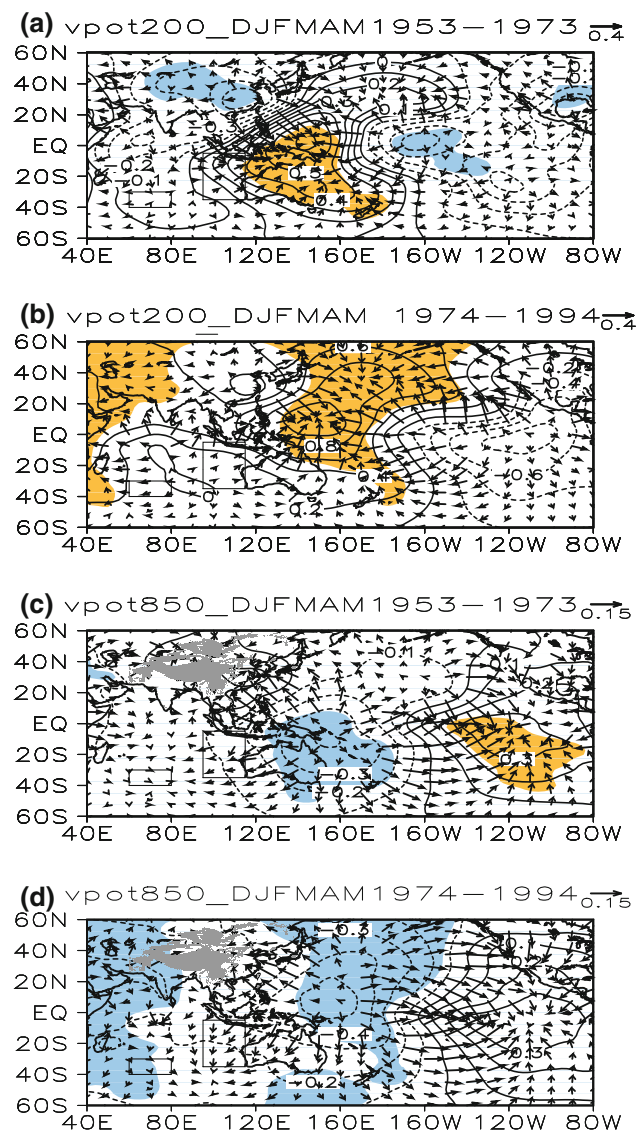


Fig. 5 Anomalies of velocity potential at 200 hPa (a, b) and 850 hPa (c, d) and the corresponding divergent winds in DJFMAM obtained by regression on normalized southern China DJFMAM rainfall during 1953–1973 (a, c) and 1974–1994 (b, d). The wind scale is shown at the top of the respective panels. Contour interval is $0.2 \times 10^6 \text{ S}^{-1}$. Shading denotes the corresponding correlation coefficient larger than 0.433, which is significant at the 95 % confidence level

over equatorial western Pacific and anomalous divergence over southern China at 200 hPa (Fig. 5a). The divergent winds flow from southern China to equatorial western Pacific, where they converge with those from equatorial central Pacific. At 850 hPa, it is obvious to observe opposite anomalies of divergence and convergence and divergent winds in the above regions (Fig. 5c). During 1974–1994, at 200 hPa, there is anomalous convergence over the western North Pacific, anomalous divergence over southern China, equatorial central Pacific, and the South Indian Ocean, with anomalous northwesterly winds from

southern China to the western North Pacific, anomalous southwesterly from the South Indian Ocean to the western North Pacific and anomalous easterlies from the equatorial central Pacific to the western North Pacific (Fig. 5b). At 850 hPa, anomalies of divergence and convergence and anomalous divergent winds are opposite in the above regions (Fig. 5d). One important feature to note for the period 1974–1994 is the divergent winds linking the South Indian Ocean and the western North Pacific. This feature is consistent with the contrast in the anomalous vertical motion (Fig. 4b) and the SST anomalies (Fig. 2b) between these two regions. Differently, the divergent winds appear to be mainly zonal in the tropics during 1953–1973. Thus, it appears that the anomalous SST is a main driver for anomalous circulation and convection over the western North Pacific and anomalous rainfall over southern China during 1953–1973, whereas during 1974–1994, the South Indian Ocean and equatorial central Pacific SST anomalies appear to act in concert and the observed anomalous circulation and convection over the western North Pacific and anomalous rainfall over southern China are likely a result of the combined effects of both the South Indian Ocean SST anomalies and ENSO.

4 Composite analysis for the influence of the South Indian Ocean SST

The analysis in the above section indicates plausible contributions of both the South Indian Ocean and equatorial central Pacific SST anomalies to southern China winter-spring rainfall variability through changes in atmospheric circulation. The regression, however, cannot determine the individual impacts of the South Indian Ocean or equatorial central Pacific SST anomalies. So, in this section, we perform a conditional composite analysis to understand how the South Indian Ocean SST anomalies affect atmospheric circulation and southern China rainfall independently.

As shown in Fig. 2b, SST anomalies during 1974–1994 display an east–west dipole pattern in the South Indian Ocean, which is termed as the South Indian Ocean dipole (SIOD) hereafter. The SIOD SST anomaly pattern is similar to that unraveled by previous studies (e.g. Behera and Yamagata 2001; Xu and Fan 2012). Previous studies mostly focus on the effect of SIOD on the climate variability in Africa (Reason et al. 2005; Mapande and Reason 2005) and Australia (England et al. 2006). In this study, we explore how the SIOD SST anomaly pattern affects southern China winter-spring rainfall anomalies. Based on the SST anomaly pattern, we define an SST index using the difference of standard SST anomalies between the region of 95° – 115°E , 5° – 35°S and the region of 60° – 80°E , 30° – 40°S . During 1974–1994, there are 5 years (1979, 1982,

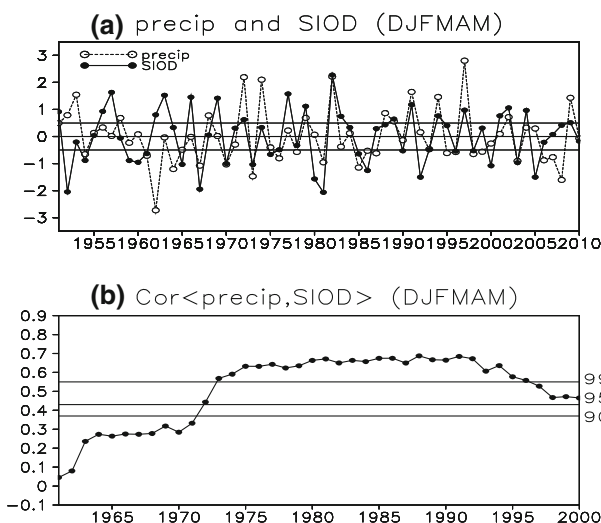


Fig. 6 **a** Time series of normalized southern China DJFMAM rainfall (open circle) and SIOD DJFMAM SST (solid circle); **b** sliding correlation between DJFMAM southern China rainfall and DJFMAM SIOD SST displayed at the center year of the 21-year window. The horizontal lines denote the 0.5 SD in Fig. 6a and the correlation coefficient at the 90, 95, 99 % confidence level in Fig. 6b

1989, 1991, 1994) in which both the SST index and southern China rainfall anomalies are more than 0.5 SD, while there are 5 years (1976, 1981, 1985, 1986, 1993) in which both the SST index and southern China rainfall anomalies are less than -0.5 SD (Fig. 6a). There are 6 in-phase years and 2 out-of-phase years during 1953–1973 based on positive or negative 0.5 SD thresholds. The relationship between the South Indian Ocean SST and southern China winter-spring rainfall becomes stronger after mid-1970s (Fig. 6b). In order to highlight the effect of SIOD during 1974–1994, it is necessary to exclude the contribution of ENSO. Cold and warm episodes of ENSO are defined when the threshold (± 0.5 °C) for the oceanic Niño index is met for a minimum of 5 consecutive overlapping seasons (cited from http://www.cpc.ncep.noaa.gov/products/analysis_monitoring/ensostuff/ensoyears.shtml). During 1974–1994, there are 7 El Niño years (1976, 1977, 1982, 1986, 1987, 1991, 1994) and 5 La Niña years (1974, 1975, 1983, 1984, 1988). We get 2 years (1979, 1989) in which both SIOD SST index and southern China rainfall anomalies are positive excluding El Niño effect and 5 years (1976, 1981, 1985, 1986, 1993) in which both SIOD SST index and southern China rainfall anomalies are negative excluding La Niña effect. In these cases, the South Indian Ocean SST anomalies contribute independently to southern China rainfall anomalies.

Figure 7 shows composite anomalies of 850 hPa winds, 200 hPa winds, 500 hPa vertical velocity and SST with negative SIOD years (1976, 1981, 1985, 1986, 1993) minus positive SIOD years (1979, 1989). The wind anomalies

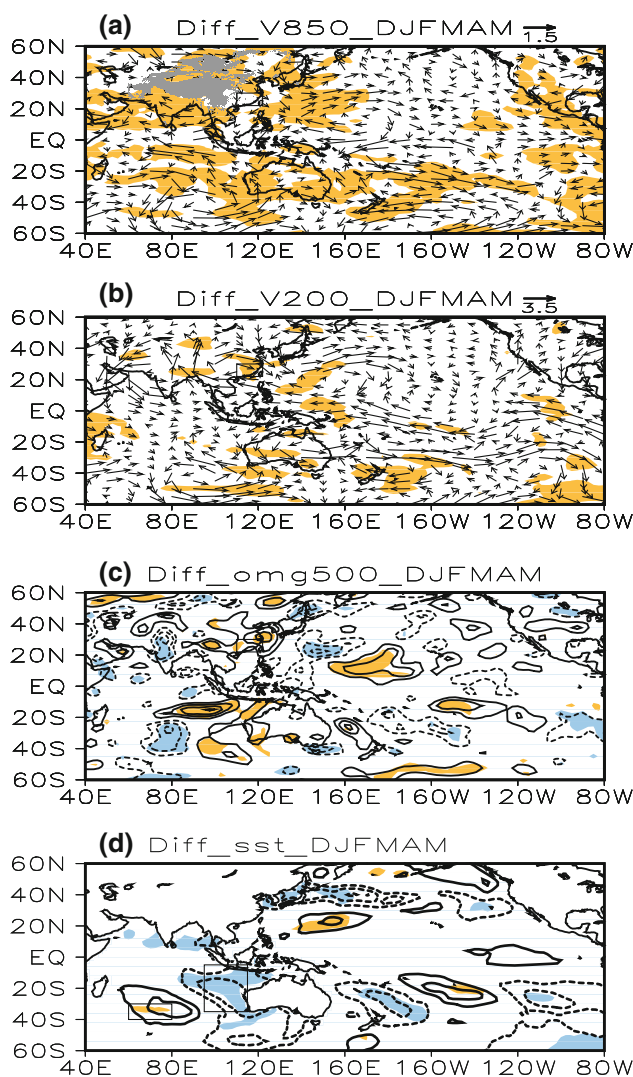


Fig. 7 Composite anomalies of 850 hPa winds (a), 200 hPa winds (b) 500 hPa p-vertical velocity (c) and SST (d) in DJFMAM for the cases that the DJFMAM SIOD SST anomalies are of the same sign as DJFMAM southern China rainfall anomalies, but excluding the ENSO cases that DJFMAM NINO3.4 SST anomalies are of the same sign as DJFMAM southern China rainfall anomalies during 1974–1994. The zero contour in (c, d) is suppressed. Contour interval is 0.006 Pa/s in (c) and 0.2 °C in (d). The shadings denote differences significant at the 90 % confidence level according to the Student's *t* test

over the South Indian Ocean feature responses to warming associated with positive SST anomalies in western South Indian Ocean and cooling associated with negative SST anomalies in eastern South Indian Ocean. There is an anomalous anticyclone at lower-level and anomalous cyclone at upper-level over the South Indian Ocean. Anomalous northerlies dominate over southern China and separate into two branches over the South China Sea, the eastward one converging with anomalous easterlies over the Philippine Sea and the westward one crossing

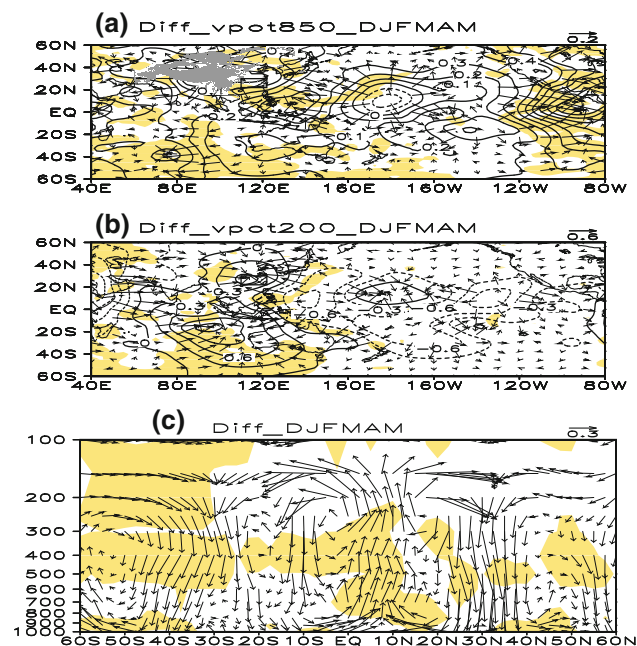


Fig. 8 Composite anomalies of DJFMAM velocity potential at 850 hPa (a) and 200 hPa (b) and corresponding divergent winds, and DJFMAM vertical circulation consisting of divergent meridional wind (m/s) and vertical p-velocity (0.01 Pa/s) along 110°–130°E (c) for the cases that the DJFMAM SIOD SST anomalies are of the same sign as DJFMAM southern China rainfall anomalies, but excluding the ENSO cases that DJFMAM NINO3.4 SST anomalies are of the same sign as DJFMAM southern China rainfall anomalies during 1974–1994. The shadings denote differences significant at the 99 % confidence level according to the Student's *t* test

Indochina to the Bay of Bengal. At 500 hPa, anomalous descent and ascent are observed over the eastern and western South Indian Ocean, respectively (Fig. 7c), featuring an east–west contrast, which is consistent with the SST contrast (Fig. 7d). There is ascent over southern South China Sea to the western North Pacific and descent over southern China and tropical central North Pacific. The equatorial central Pacific SST anomalies are weak, which confirms that the ENSO effect is weak for the selected cases.

The above circulation anomalies suggest a close connection between the atmospheric circulation over southern China and that over the South Indian Ocean. A similar connection has been found in summer (Wu et al. 2012). To further understand the connection between the South Indian Ocean SST and southern China circulation, we show in Fig. 8 anomalies of velocity potential at 200 and 850 hPa obtained by composite analysis with negative SIOD years minus positive SIOD years. At 850 hPa, there is anomalous divergence over southern China, anomalous convergence over the western North Pacific, and anomalous divergence over the South Indian Ocean (Fig. 8a). The divergent winds flow from the South Indian Ocean to the

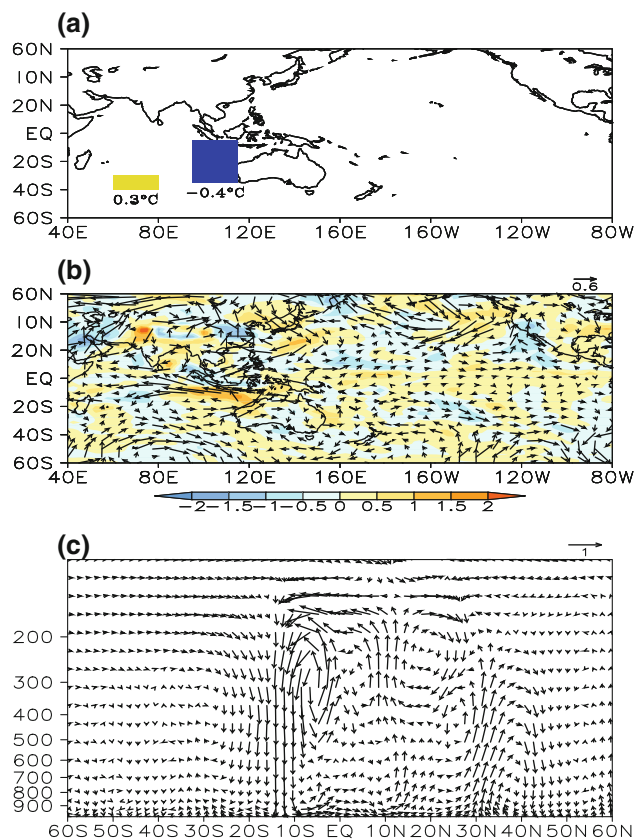


Fig. 9 SST anomaly distribution for the SIOD SST experiment (a), composite differences in DJFMAM of (b) 850 hPa winds (vector), 500 hPa p-vertical velocity (shading) and (c) vertical circulation consisting of divergent meridional wind (m/s) and vertical p-velocity (0.01 Pa/s) along 110°–130°E between experiments of negative SIOD and CAM4 control

western North Pacific, where they converge with those from southern China. Anomalies of divergence and convergence and the divergent winds at 200 hPa are opposite to those at 850 hPa (Fig. 8b).

The above features suggest an anomalous cross-equatorial vertical circulation between the South Indian Ocean and the western North Pacific and another anomalous vertical cell between the western North Pacific and southern China, similar to the feature identified for summer (Wu et al. 2012). This is further demonstrated in Fig. 8c. Obviously, there are two vertical cells between the South Indian Ocean and southern China with a common branch over the South China Sea (Fig. 8c).

In order to confirm the impact of the South Indian Ocean SST anomalies independent of ENSO on southern China winter-spring rainfall, we carry out two experiments using the NCAR CAM4 model. In the experiments, CAM4_control is run for 20 years with climatological mean seasonal cycle of SST forcing in the global ocean and the outputs over the last 10 years are used in the analysis. The 10-year mean winter-spring values are equivalent to

those from an ensemble of 10 sensitivity experiments changing the South Indian Ocean SST using different initial atmospheric and land surface conditions (Zhao et al. 2010). We focus on the positive and negative anomalous centers of South Indian Ocean SST (shown in Fig. 2b). Experiment SIO_SST is the same as CAM4_control except for a decrease of $-0.4\text{ }^{\circ}\text{C}$ in SST in the region of $5\text{--}35^{\circ}\text{S}$ and $95\text{--}115^{\circ}\text{E}$ and an increase of $0.3\text{ }^{\circ}\text{C}$ in SST in the region of $30\text{--}40^{\circ}\text{S}$ and $60\text{--}80^{\circ}\text{E}$ under the background of climatological mean seasonal cycle of SST (Fig. 9a).

Corresponding to the decrease in DJFMAM SST over eastern South Indian Ocean and increase in DJFMAM SST over western South Indian Ocean between experiments SIO_SST and CAM4_Control, anomalous anticyclones at lower-level are seen over the South Indian Ocean and eastern China to East China Sea. The westerly anomalies over southern South China Sea converge over the western North Pacific with the easterly anomalies along the south flank of eastern China-East China Sea anticyclone. Anomalous ascending motion dominates over the western North Pacific, while anomalous descending motion is over southern China and eastern South Indian Ocean (Fig. 9b). Latitude-altitude cross-section of anomalous vertical motion and meridional divergent winds averaged along $110^{\circ}\text{--}130^{\circ}\text{E}$ show that there are two anomalous vertical circulations between the South Indian Ocean and southern China (Fig. 9c). The ascending branch lies over the western North Pacific and descending is seen over the South Indian Ocean and southern China though the descending motion over southern China is weaker than that in Fig. 8c. Those features indicate that the South Indian Ocean SST anomalies can affect southern China winter-spring rainfall through vertical cells.

While the results of numerical experiments broadly support the impact of the South India Ocean SST anomalies on southern China winter-spring rainfall, there are notable differences from observations. In particular, anomalous vertical motion around 30°N over eastern China in the model experiment is opposite to the observations (Fig. 9b versus Fig. 7c). In consequence, anomalous downward motion is limited to the coastal region of southern China in the model (Fig. 9b).

5 Discussions of reasons for interdecadal change in the rainfall-SST relationship

In addressing the reasons for the interdecadal change in the southern China summer rainfall-SST relationship, Wu et al. (2012) pointed out the plausible influence of changes in the mean state and in the location and magnitude of SST anomalies in the southeastern Indian Ocean. The mean state change may shift the location of the mean western

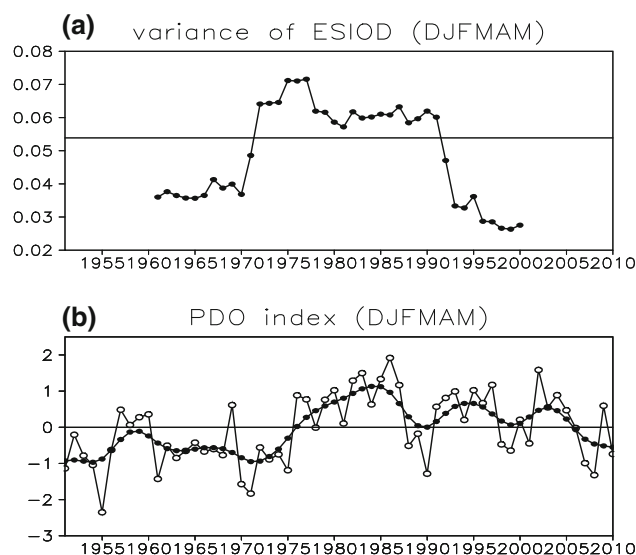


Fig. 10 **a** Moving variance of DJFMAM eastern South Indian Ocean SST ($5^{\circ}\text{--}35^{\circ}\text{S}$, $95^{\circ}\text{--}115^{\circ}\text{E}$) with a 21-year window. The variance is shown at the center year of the 21-year window. The solid line is the mean variance. **b** Time series of DJFMAM PDO index (open circle) and PDO index with 9-year moving average (solid circle)

North Pacific subtropical high, which in turn displaces the location of anomalous rainfall region. The change in the location and magnitude of southeastern Indian Ocean SST anomalies may lead to a change in the affected region and the magnitude of these SST forcing.

Here, we show in Fig. 10a the moving variance of eastern South Indian Ocean SST ($5\text{--}35^{\circ}\text{S}$, $95\text{--}115^{\circ}\text{E}$) in winter-spring with a 21-year window. Clearly, the South Indian Ocean SST variance is significantly larger after the mid-1970s than before the mid-1970s. The South Indian Ocean SST variance is about 0.06 during 1974–1994 and 0.036 during 1953–1973, respectively. This indicates a stronger forcing of the South Indian Ocean SST anomalies after the mid-1970s than before the mid-1970s. Thus, the South Indian Ocean SST anomalies and ENSO may act in concert, through modulating the western North Pacific circulation, to contribute to southern China winter-spring rainfall variability during 1974–1994. Note that the variance of the western pole of the SIOD SST anomaly pattern displays a linear decreasing trend during the 1960s through mid-1970s and remains nearly at the same magnitude after that (figure not shown). As such, the SIOD index variance showed an increase in the mid-1970s (figure not shown) as that of the eastern South Indian Ocean SST anomalies.

Another plausible reason for the change in the southern China winter-spring rainfall-ENSO relationship may be the interdecadal modulation of Pacific decadal oscillation (PDO) upon the impact of ENSO on southern China winter-spring rainfall. ENSO affects the East Asian climate through a Pacific-east Asian teleconnection featuring an

anomalous anticyclone over the Philippine Sea and anomalous southwesterly winds along its northwest flank during the mature and decay phases of El Niño events (Wang et al. 2000). These anomalous southwesterlies enhance the moisture supply to southern China, leading to above-normal rainfall there (Zhang et al. 1996; Wang et al. 2000; Wu et al. 2003). Wang et al. (2008a, 2008b) proposed that the relationship between ENSO and EAWM depended on the phase of PDO. The interannual relationship between ENSO and EAWM is weak and insignificant in the high phase of PDO. In contrast, ENSO exerts a strong impact on EAWM in the low phase of the PDO. This is attributed to the PDO's modulation of the anomalous Philippine Sea anticyclone. The anomalous Philippine Sea anticyclone is located more northwestward in the low phase of PDO than in the high phase of PDO. As such, associated southwesterly winds are more likely to affect southern China in the low phase of PDO. As shown in Fig. 10b, the PDO is in the low phase during 1953–1973 and in the high phase during 1974–1994, respectively. The observed weakening of the relationship between ENSO and southern China winter-spring rainfall appears to be consistent with the phase change in the PDO. Gollan et al. (2012) suggested that tropical forcing is an important source for the EAWM variability by modulating circulation anomalies in the tropical Pacific and Indian Ocean. The results obtained in this study are broadly consistent with Gollan et al. (2012) regarding the role of tropical SST anomalies. However, our results indicate that the specific tropical region influencing the winter-spring southern China precipitation has changed with the effect of ENSO and South Indian Ocean SST anomalies dominating alternatively during 1953–1973 and 1974–1994, respectively.

6 Summary

The relationship of southern China winter-spring rainfall with ENSO experienced an obvious change around the mid-1970s. Before the mid-1970s, the southern China winter-spring rainfall tends to be more (less) than normal during the El Niño (La Niña) years, whereas after the mid-1970s, this relationship is weakened. Accompanying this change, above-normal southern China winter-spring rainfall follows warmer SST in eastern South Indian Ocean and colder SST in western South Indian Ocean during the mid-1970s through the mid-1990s.

Different features in the ocean and the atmospheric anomalies associated with southern China winter-spring rainfall between two periods are identified in this study. During 1953–1973, there are two cells between the equatorial central Pacific and southern China: one

between the equatorial central Pacific and the western North Pacific and the other between the western North Pacific and southern China, with a common branch over the western North Pacific as a connection. During 1974–1994, there are two meridional cells between the South Indian Ocean and southern China: one between the South Indian Ocean and the western North Pacific and the other between the western North Pacific and southern China, with a common branch over the western North Pacific acting as a link. As such, anomalous heating induced by positive equatorial central Pacific SST anomalies is accompanied by anomalous ascent and above-normal rainfall over southern China in the former period, while anomalous heating induced by positive SST anomalies in western South Indian Ocean and negative SST anomalies in eastern South Indian Ocean leads to anomalous descent and below-normal rainfall over southern China.

The South Indian Ocean SST anomalies can affect atmospheric circulation and rainfall over southern China independently based on the composite analysis and model experiment. In comparison, there are more cases of cooler SST in eastern South Indian Ocean and warmer SST in western South Indian Ocean independently causing the winter-spring southern China drought than the opposite situation. The change in the relationship between southern China winter-spring rainfall and ENSO may be related to changes in the variance of the South Indian Ocean SST anomalies and in the phase of PDO. The magnitude of eastern South Indian Ocean SST anomalies experienced a significant increase around the mid-1970s, enhancing the role of the South Indian Ocean SST forcing in atmospheric circulation and rainfall anomalies. The PDO experienced a phase change from low to high, weakening the influence of ENSO after the mid-1970s through its modulation of the Pacific-east Asian teleconnection.

In addition to the weakening of the correlation around the late 1970s, Fig. 1b displays a strengthening of the correlation between southern China rainfall and NINO4 SST in the late 1990s. What is the implication of this strengthening correlation and what is the cause for this change are interesting questions, but these are beyond the scope of this study.

The present study is mostly based on correlation and regression analysis. The number of cases for the independent influences of the South Indian Ocean SST anomalies is limited. While we have performed numerical experiments to confirm the influence of the South Indian Ocean SST anomalies, these experiments are idealized. Thus, further studies with longer data and more systematic numerical experiments will be needed in the future to validate the conclusions obtained in this study.

Acknowledgments This research is jointly supported by the National Key Basic Research Program of China (Grant No. 2009CB421404), the National Natural Science Foundation of China (Grant No. 41175076), the Fundamental Research Funds for the Central Universities (Grant No. 111gc10), and the National Natural Science Foundation of China (Grant No. 412111046). R. Wu acknowledges the support of a Direct Grant of the Chinese University of Hong Kong (Grant No. 2021105), a Hong Kong Research Grants Council grant (CUHK403612), and the National Natural Science Foundation grants (41275081 and 41228006). The authors thank Auroral 5000A high performance computing platform of Sun Yat-Sen University for providing a convenience for running model CAM4.

References

- Behera SK, Yamagata T (2001) Subtropical SST dipole events in the southern Indian Ocean. *Geophys Res Lett* 28:327–330
- Chen LT, Wu R (2000) Interannual and decadal variations of snow cover over Qinghai-Xizang Plateau and their relationships to summer monsoon rainfall in China. *Adv Atmos Sci* 17:18–30
- Chen LT, Yan ZX (1979) Impact of Himalayan winter–spring snow cover on atmospheric circulation and southern China rainfall in the rainy season (in Chinese). In Yangtze River Regulating Office(ed) *Collected Papers on Medium and Long-Term Hydrological and Meteorological Forecasts*, vol. 1, Water Conservancy and Power Press, pp 185–194
- Chen W, Wang L, Xue Y, Sun S (2009) Variabilities of the spring river runoff system in eastern China and their relations to precipitation and sea surface temperature. *Int J Climatol* 29:1381–1394
- England MH, Ummenhofer CC, Santoso A (2006) Interannual rainfall extremes over southwest Western Australia linked to Indian Ocean climate variability. *J Clim* 19:1948–1969
- Gao H, Chen L, Jia X, Ke Z, Han R, Zhang P, Wang Q, Sun C, Zhu Y, Li W, Sun L, Ren F, Wang L, Gao G (2008) Analysis of the severe cold surge, ice-snow and frozen disasters in South China during January 2008: II. Possible climate causes (in Chinese). *Meteor Mon* 34:101–106
- Gollan G, Greatbatch RJ, Jung T (2012) Tropical impact on the East Asian winter monsoon. *Geophys Res Lett* 39:L17801. doi:10.1029/2012GL052978
- Gong DY, Wang SW, Zhu JH (2001) East Asian winter monsoon and arctic oscillation. *Geophys Res Lett* 28:2073–2076
- He XC, Ding YH, He JH, Li QP (2007) Analysis on anomalous precipitation in southern China during winter monsoons. *Acta Meteor Sin* 21:385–396
- Huang RH, Chen JL, Wang L, Lin ZD (2012) Characteristics, processes, and causes of the spatio-temporal variabilities of the East Asian monsoon system. *Adv Atmos Sci* 29(5):910–942. doi:10.1007/s00376-012-2015-x
- Inoue T, Matsumoto J (2004) A comparison of summer sea level pressure over East Eurasia between NCEP-NCAR reanalysis and ERA-40 for the period 1960–99. *J Meteor Soc Japan* 82:951–958
- Kalnay E, Kanamitsu M, Kistler R, Collins W, Deaven D, Gandin L, Iredell M, Saha S, White G, Woollen J, Zhu Y, Leetmaa A, Reynolds R, Chelliah M, Ebisuzaki W, Higgins W, Janowiak J, Mo KC, Ropelewski C, Wang J, Jenne R, Joseph D (1996) NCEP/NCAR 40-year reanalysis project. *Bull Am Meteor Soc* 77:437–471
- Li XZ, Liang W, Wen ZP (2010) Characteristics of the atmosphere water vapor and its relationship with rainfall in south China in northern autumn, winter and spring (in Chinese). *J Tropical Meteor* 26:626–632. doi:1004-4965(2010)05-0626-07
- Liu XD, Wang Y (2011) Contrasting impacts of spring thermal conditions over Tibetan Plateau on late-spring to early-summer precipitation in Southeast China. *Atmos Sci Lett* 12:309–315
- Ma ZJ (2009) A retrospective study of the 2008 huge disaster by low temperature, snow and ice in South China (in Chinese). *J Nat Disasters* 18:1–3
- Mapande AT, Reason CJC (2005) Links between rainfall variability on intra seasonal and interannual scales over western Tanzania and regional circulation and SST patterns. *Meteor Atmos Phys* 89:215–234
- Neale R B, Richter JH, Conley AJ, Park S, Laurizen PH, Gettelman A, Williamson DL, Rasch PJ, Taylor MA, Collins WD, Zhang M, Lin SJ (2011) Description of the NCAR Community Atmosphere Model (CAM4). Tech. Rep. NCAR/TN-485 + STR, National Center for Atmospheric Research. 6 pp
- Rayner NA, DE Parker, Horton EB, Folland CK, Alexander LV, Rowell DP, Kent EC, Kaplan A (2003) A Global analyses of sea surface temperature, sea ice, and night marine air temperature since the late nineteenth century. *J Geophys Res* 108(D14):4407. doi:10.1029/2002JD002670
- Reason CJC, Hachigonta S, Phaladi RF (2005) Interannual variability in rainy season characteristics over the Limpopo region of southern Africa. *Int J Climatol* 25:1835–1853
- Smith TM, Reynolds RW, Peterson TC, Lawrimore J (2008) Improvements to NOAA’s historical merged land-ocean surface temperature analysis (1880–2006). *J Clim* 21:2283–2296
- Sun C, Yang S (2012) Persistent severe drought in southern China during winter–spring 2011: large-scale circulation patterns and possible impacting factors. *J Geophys Res* 117:D10112. doi:10.1029/2012JD017500
- Sung MK, Lim GH, Kug JS (2010) Phase asymmetric downstream development of the North Atlantic oscillation and its impact on the East Asian winter monsoon. *J Geophys Res* 115:D09105. doi:10.1029/2009JD013153
- Wang L, Feng J (2011) Two major modes of the wintertime precipitation over China. *Chinese J Atmos Sci* 35:1105–1116
- Wang B, Wu R, Fu XH (2000) Pacific–East Asia tele connection: how does ENSO affect East Asian climate? *J Clim* 13:1517–1536
- Wang B, Wu R, Li T (2003) Atmosphere–warm ocean interaction and its impact on Asian–Australian monsoon variation. *J Clim* 16:1211–11595
- Wang L, Gao G, Zhang Q, Sun J, Wang Z, Zhang Y, Zhao S, Chen X, Chen Y, Wang Y, Chen L, Gao H (2008a) Analysis of the severe cold surge, ice-snow and frozen disasters in South China during January 2008: I. Climatic Features and Its Impact (in Chinese). *Meteor Mon* 34:95–100
- Wang L, Chen W, Huang R (2008b) Interdecadal modulation of PDO on the impact of ENSO on the East Asian winter monsoon. *Geophys Res Lett* 35:L20702. doi:10.1029/2008GL035287
- Wang T, Yang S, Wen Z, Wu R, Zhao P (2011) Variations of the winter India–Burma trough and their links to climate anomalies over southern and eastern Asia. *J Geophys Res* 116:D23118. doi:10.1029/2011JD016373
- Wen M, Yang S, Kumar A, Zhang P (2009) An analysis of the large scale climate anomalies associated with the snowstorms affecting China in January 2008. *Mon Weather Rev* 137:1111–1131
- Wu BY, Huang RH (1999) Effects of the extremes in the North Atlantic oscillation on East Asia winter monsoon. *Chinese J Atmos Sci* 23:641–651
- Wu R, Kirtman BP (2007a) Observed relationship of spring and summer East Asia rainfall with winter and spring Eurasian snow. *J Clim* 20:1285–1304
- Wu R, Kirtman BP (2007b) Regimes of seasonal air–sea interaction and implications for performance of forced simulations. *Clim Dyn* 29:393–410. doi:10.1007/s00382-007-0246-9
- Wu R, Wang B (2000) Interannual variability of summer monsoon onset over the western North Pacific and the underlying processes. *J Clim* 13:2483–2501

- Wu BY, Wang J (2002a) Possible impacts of winter Arctic oscillation on Siberian High, the East Asian winter monsoon and sea-ice extent. *Adv Atmos Sci* 19:297–320
- Wu BY, Wang J (2002b) Winter Arctic oscillation, Siberian High and East Asian winter monsoon. *Geophys Res Lett* 29:1897. doi:[10.1029/2002GL015373](https://doi.org/10.1029/2002GL015373)
- Wu R, Hu ZZ, Kirtman BP (2003) Evolution of ENSO-related rainfall Anomalies in East Asia. *J Clim* 16:3742–3758
- Wu R, Kinter JL III, Kirtman BP (2005) Discrepancy of interdecadal changes in the Asian region among the NCEP-NCAR reanalysis, objective analyses, and observations. *J Clim* 18:3048–3067
- Wu R, Yang S, Liu S, Sun L, Yi L, Gao Z (2010) Changes in the relationship between Northeast China summer temperature and ENSO. *J Geophys Res* 115:D21107. doi:[10.1029/2010JD014422](https://doi.org/10.1029/2010JD014422)
- Wu R, Yang S, Wen Z, Huang G, Hu K (2012) Interdecadal change in the relationship of southern China summer rainfall with tropical Indo-Pacific SST. *Theor Appl Climatol* 108:119–133. doi:[10.1007/s00704-011-0519-4](https://doi.org/10.1007/s00704-011-0519-4)
- Xu ZQ, Fan K (2012) Possible process for influences of winter and spring Indian Ocean SST anomalies interannual variability mode on summer rainfall over eastern China. *Chinese J Atmos Sci* 36:879–888. doi:[10.3878/j.issn.1006-9895.2012.11176](https://doi.org/10.3878/j.issn.1006-9895.2012.11176)
- Yang Q (2009) Impact of the Indian Ocean subtropical dipole on the precipitation of east China during winter monsoons. *J Geophys Res* 114:D14110. doi:[10.1029/2008JD011173](https://doi.org/10.1029/2008JD011173)
- Yang H (2011) The significant relationship between the Arctic oscillation (AO) in December and the January climate over South China. *Adv Atmos Sci* 28:398–407. doi:[10.1007/s00376-010-0019-y](https://doi.org/10.1007/s00376-010-0019-y)
- Yang S, Lau KM, Kim KM (2002) Variations of the East Asian jet stream and Asian-Pacific-American winter climate anomalies. *J Clim* 15:306–325
- Zhang R, Sumi A (2002) Moisture circulation over East Asia during El Niño episode. *J Meteor Soc Japan* 80:213–227
- Zhang RH, Sumi A, Kimoto M (1996) Impact of El Niño on the East Asian monsoon: a diagnostic study of the 86/87 and 91/92 events. *J Meteor Soc Japan* 74:49–62
- Zhang R, Sumi A, Kimoto M (1999) A diagnostic study of the impact of El Niño. *Adv Atmos Sci* 16:229–241
- Zhang Z, Gong D, Hu M, Guo D, He X, Lei Y (2009) Anomalous winter temperature and precipitation events in southern China. *J Geogr Sci* 19:471–488. doi:[10.1007/s11442-009-0471-8](https://doi.org/10.1007/s11442-009-0471-8)
- Zhao LN, Ma QY, Yang GM, Wang XR, Zhao XR, Lu Q, Yang XD, Wu H, Wang Z, Kang ZM, Mao DY (2008) Disasters and its impacts of a severe snow storm and freezing rain over southern China in January 2008 (in Chinese). *Climatic Environ Res* 13:556–566
- Zhao P, Cao Z, Chen J (2010) A summer teleconnection pattern over the extratropical Northern Hemisphere and associated mechanisms. *Clim Dyn* 35:523–534. doi:[10.1007/s00382-009-0699-0](https://doi.org/10.1007/s00382-009-0699-0)
- Zhou L, Wu R (2010) Respective impacts of East Asia winter monsoon and ENSO on winter rainfall in China. *J Geophys Res* 115:D02107. doi:[10.1029/2009JD012502](https://doi.org/10.1029/2009JD012502)
- Zhou L, Tam CY, Zhou W, Chan JCL (2010) Influence of South China Sea SST and the ENSO on winter rainfall over South China. *Adv Atmos Sci* 27:832–844
- Zhou BZ et al (2011) The Great 2008 Chinese Ice Storm: its Socioeconomic–Ecological Impact and Sustainability Lessons Learned. *Bull Am Meteor Soc* 92:47–60. doi:[10.1175/2010BAMS2857.1](https://doi.org/10.1175/2010BAMS2857.1)
- Zong HF, Bueh C, Wei J, Chen LT (2012) Intensity of the trough over the Bay of Bengal and its impact on the Southern China precipitation in winter. *Atmos Oceanic Sci Lett* 5:246–251